Steam reforming of tar using biomass gasification char in a Pilot-scale gasifier

Ali Abdelaal, Daniele Antolini, Stefano Piazzi, Francesco Patuzzi, Audrey Villot, Claire Gerente, Marco Baratieri

Fuel 351 (2023) 128898

Contents lists available at ScienceDirect

Fuel

journal homepage: www.elsevier.com/locate/fuel

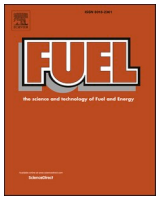

Full Length Article

Steam reforming of tar using biomass gasification char in a Pilot-scale gasifier

Ali Abdelaal [a,b,*], Daniele Antolini [a], Stefano Piazzi [a], Francesco Patuzzi [a], Audrey Villot [b], Claire Gerente [b], Marco Baratieri [a]

[a] Free University of Bozen-Bolzano, Faculty of Engineering, Piazza Domenicani 3, 39100 Bolzano, Italy
[b] IMT Atlantique, GEPEA UMR CNRS 6144, F-44307 Nantes, France

ARTICLE INFO

Keywords:
Catalysis
Circular economy
Gas upgrading
Gasification chars
Tar reforming

ABSTRACT

Gasification char is a residual material produced during the biomass gasification process. Considered as industrial waste, it is typically disposed of through incineration or landfilling, thereby incurring significant economic costs. Nonetheless, gasification char is characterized by its high carbon content and surface area making it an economical alternative to common catalysts and catalyst support materials. In this study, char from a pilot-scale downdraft gasifier was used to reform the tar generated from the same gasifier. Reforming was performed both in the presence and absence of steam. The aim is to convert condensable hydrocarbon derivatives (tars) into non-condensable lower molecular weight products such as H_2 and CO. Reforming test conducted with 0.18 kg/h steam for 2 h at 750 °C and char bed weighing 600 g resulted in a reduction of tar concentration from 2407 mg/Nm^3 to 20 mg/Nm^3. The same test conditions were also responsible for an increase in H_2 production from 15 to 26 vol%. The combined effect of steam and char bed suggests that both upgrading the producer gas as well as cleaning it can be made possible in a single process.

1. Introduction

In 2017, Europe's consumption of woody biomass for bioenergy production was estimated at 424 million m^3 [1]. Sustainably sourced biomass is a very attractive renewable energy source facilitating the transition towards climate neutrality. Multiple processes such as gasification can harness the chemical energy stored in biomass by the conversion into a gas rich in carbon monoxide (CO) and hydrogen (H_2), as well as biofuels and other valuable by-products. The generated gas is called synthesis gas or syngas that can be implemented directly in diesel engines, or used for electricity and heat generation. It is also possible to separate the H_2 from the syngas to be burned or used in fuel cells. Additionally, the syngas can be converted into liquid fuels through Fischer–Tropsch process [2–4]. This pathway where biomass is transformed into syngas and then into biofuels offers a means towards renewable energy storage making the gasification process even more attractive [5,6]. Currently, over 1500 small-scale gasification plants operating worldwide that generate syngas mainly for heat or combined heat and power (CHP) production [7]. At large-scale, gaseous or liquid biofuels production or co-firing is more common. Various types of biomass gasifiers exist but the most widespread are downdraft gasifiers. Newer technologies such as updraft, double-fired, floating bed, and gasifiers with hot gas filtering are gaining momentum. The scale of operation has also grown significantly, from around 180 kWel up to 1 MWel, leading to an increased volume of by-products, such as tar and char [8].

Gasification char is a solid carbonaceous material accounting for nearly 10 % of the original gasifier feedstock [9]. It is an industrial waste that requires proper disposal and handling at a nonnegligible cost which can impact the economic viability of a plant. Chars can exhibit unique features in terms of chemical composition (high carbon and mineral content), or physical properties (high porosity and surface area) leading to various potential applications. For instance, gasification char produced from woody biomass tends to have a larger surface area and higher carbon content [10]. The high process temperature typical of gasification results in the loss of some inorganics (e.g., Zn, Cd, As, Se, K, and Na) [11]. It also results in the loss of functional groups and a smaller fraction of aromatic C-H groups [12,13]. This is a major variation between gasification and pyrolysis char. Nevertheless, gasification char has a high degree of aromaticity and environmental stability. The major

* Corresponding author at: Free University of Bozen-Bolzano, Faculty of Engineering, Piazza Domenicani 3, 39100 Bolzano, Italy.
E-mail address: ali.abdelaal@outlook.com (A. Abdelaal).

https://doi.org/10.1016/j.fuel.2023.128898
Received 31 January 2023; Received in revised form 27 May 2023; Accepted 2 June 2023
Available online 8 June 2023

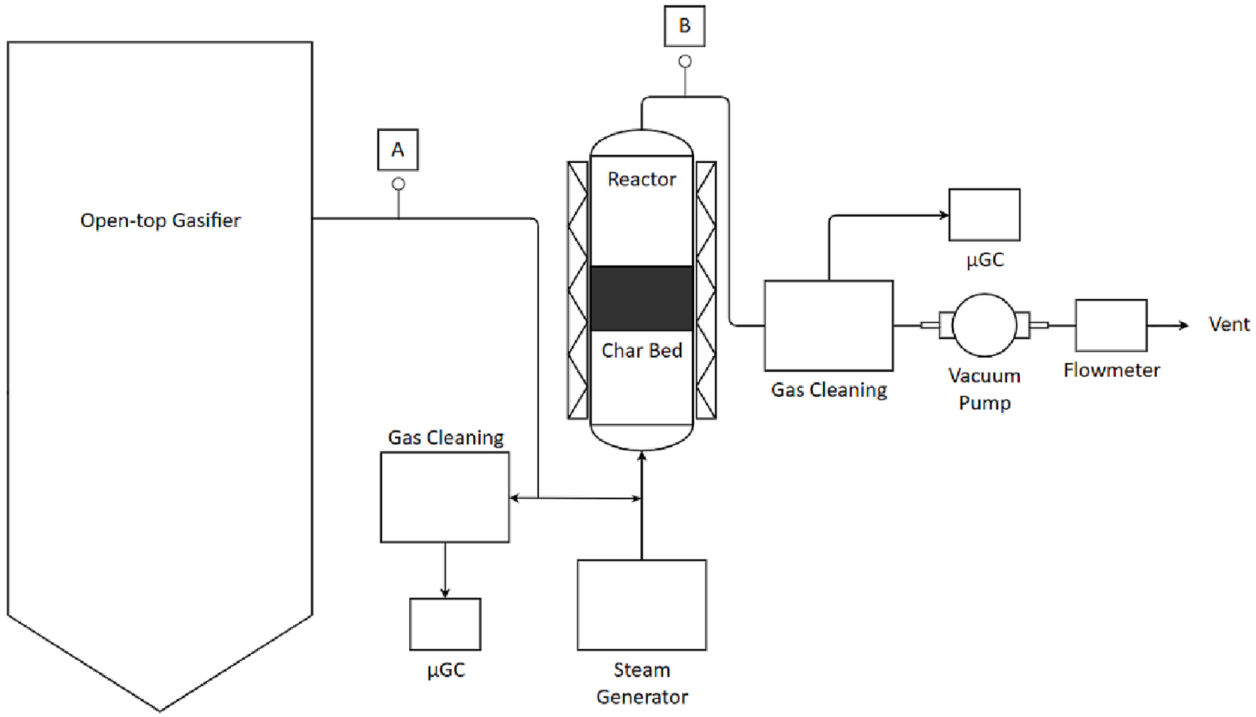

Fig. 1. Pilot-scale tar reforming setup.

char qualities found in catalysis and tar reforming applications are high surface area and the presence of inorganics with catalytic effects [14,15]. Additionally, the weak base nature of gasification char makes it highly resistant to deactivation caused by coke and heavy metals deposition [16]. Recently, char attracted more attention in the field of tar reforming due to its sustainable sourcing and low preparation cost [16–19]. It was the second most common application of gasification char after adsorption according to a recent review [20].

Tar is characterized by its black or brown color, and liquid or viscous semi-solid nature. It consists of complex mixtures of polycyclic aromatic hydrocarbons (PAH), phenolic compounds, and heterocyclic compounds [21]. It is another by-product of the gasification process. Tar reduction can be achieved through cracking and reforming reactions. This can be further classified based on the tar reduction environment (with or without steam). Thermal and steam cracking break down the tar into smaller hydrocarbons. Thermal cracking usually requires elevated temperatures (>1100 °C) with the addition of oxygen. It is considered an energy-intensive process. In the case of steam cracking, tar is mixed with steam in the absence of oxygen to form lighter tar compounds. On the other hand, the reforming reactions converts tar into simpler molecules such as H_2 and CO [22]. The simplified dry and steam reforming reactions (1) and (2) are listed below.

$$C_nH_x + nH_2O \rightarrow (n + x/2)H_2 + nCO \quad (1)$$

$$C_nH_x + nCO_2 \rightarrow (x/2)H_2 + 2nCO \quad (2)$$

Both cracking and reforming can be enhanced using a catalyst. Common catalysts used in tar reduction are dolomite, alkali metal, and nickel [23]. Another possibility of tar reduction is through the coke deposition on the char surface as shown in reactions (3) and (4) [24].

$$C_nH_x \rightarrow C_nH_m + coke/soot + gas \quad (3)$$

$$C_nH_x + H_2 \leftrightarrow CO + H_2 + CH_4 + \ldots + coke/soot \quad (4)$$

Therefore, char presents a versatile material that could promote the transition towards a circular economy, according to which, the'end-of-life' notion is replaced by reducing, reusing, recycling, and recovering materials in the production, distribution, and consumption phases [25]. In addition to the environmental benefits, char valorization could also increase the economic viability of large-scale gasification processes [26]. In 2020, the gasification char market have seen a 70 % growth rate [27] and recently, its utilization has been largely regarded as a model for closing the loop in the sustainable energy field [28].

Despite its numerous advantages, previous tar reforming studies utilizing gasification char were performed at a laboratory scale with model tar compounds [19,29–34]. Most recently, there has been a call to understand the interactions of realistic tar mixtures [35]. To the best of the authors' knowledge, the only study conducted at pilot-scale extracted real producer gas immediately after the gasifier outlet and was successful in reducing the tar content from 25 g/Nm^3 to 3.6 g/Nm^3 through ex-situ tar reformer unit without steam injection [36]. The novelty of this work lies in investigating the performance of gasification char in dry and steam reforming at a pilot-scale gasifier. Moreover, the tar reformer is connected downstream of the gasifier's cleaning stages (cyclone, water scrubbers, moisture trap) to achieve extremely low tar concentrations for sensitive applications like the Fischer-Tropsch process or fuel cells with minimal modifications of existing systems. Finally, this study is driven by the principle of circular economy which ensures process circularity. In the present work, process by-product or waste is turned into a useful material that enhances the process itself.

2. Materials and methods

2.1. Char production

The char used in this study is generated from a pilot-scale open-top downdraft gasification plant at the Bioenergy and Biofuel Lab of the Free University of Bolzano, Italy. The reactor is 1000 mm in length and 130 mm in diameter with a double-stage air feeding. The producer gas passes through a series of cleaning stages consisting of a cyclone, three scrubbers, a moisture trap, and a fabric filter before it moves to the blower and then the flare. The maximum temperature observed at the partial oxidation zone is 1100 °C. The char used in this study is collected at the bottom of the reactor. More details about the gasifier are described

Table 1
Overview of the experimental conditions.

	Temperature	Steam	Gas type	Bed weight	Bed height	Test duration
	°C	kg/h		g	mm	h
DR	750	0	Producer gas	600	145	2
SR1		0.02				
SR2		0.18				

elsewhere [15]. The plant operates on standard wood pellets (softwood) fed at a rate of 4 kg/h, using air as a gasifying agent. The moisture content, and ash content of the wood pellets were 7.56 %, and 0.23 %, respectively. While the CHNSO composition of the wood pellets were 50.02 %, 6.03 %, 0.08 %, 0.27 %, and 43.37 %, respectively [15].

2.2. Char characterization

Different characterization techniques were implemented to investigate the chemical composition and surface properties of the char before and after the tar reforming experiment. The proximate analysis (VM: volatile matter, FC: fixed carbon, and ash) was performed in triplicates by thermogravimetric analysis (TGA). The samples were first dried at 105 °C, then heated in a nitrogen atmosphere up to 950 °C, followed by combustion in air at 550 °C. The elemental composition (CHNS) was performed in triplicates using an elemental analyzer (Vario MACRO cube, Elementar). Other elements such as Na, K, and Ca were detected using X-ray fluorescence (XRF, SHIMADZU EDX-800HS). Moisture was determined by oven-drying at 105 °C. Ash content was performed by combustion in a muffle furnace at 550 °C. Both moisture and ash analyses were done in triplicates. The surface properties were measured via nitrogen adsorption–desorption at 77 K. The Brunauer-Emmet-Teller (BET) theory was used to measure the surface area with an error of 0.1–0.3 $m^2\ g^{-1}$. The mesopore and micropore volumes were determined using Barrett-Joyner-Halenda (BJH), and Horvath–Kawazoe (HK) theories, respectively. Before analysis, samples were vacuum degassed at 350 °C for 24 h. Surface area (including pore volume) analyses were done at least in duplicates. To measure the char deactivation after the reforming tests, the thermal degradation of raw (before reforming) and spent (after reforming) char samples were tested in both N_2 and synthetic air atmospheres using a thermogravimetric analyzer. Approximately 8 mg per sample were heated from 20 to 900 °C and the rate of thermal degradation was assessed. Surface morphology of the raw and spent chars was studied by scanning electron microscopy (SEM) with energy-dispersive X-ray spectroscopy (EDX) using ZEISS Merlin® FE-SEM instrument. Finally, the PAH content of the raw and spent char was evaluated by gas chromatography (GC) following the NF EN 17503 standard. The analysis was performed by SOCOR Laboratories, Dechy, France, and identified the 16 PAH compounds as per the United States Environmental Protection Agency (EPA).

2.3. Tar reforming

The tar reforming setup consisted of a cylindrical stainless-steel reactor (height: 1500 mm, internal diameter: 150 mm) that is electrically heated as shown in Fig. 1. The grate that supports the char bed is placed 500 mm from the bottom of the tube. The height of the fixed char bed was 145 mm in all experiments. The temperature profile inside the reformer is monitored using three K-type thermocouples placed at 50, 150, and 250 mm from the bottom of the bed. The producer gas is extracted at the gasifier outlet, after passing through a series of cleaning stages (cyclone, water scrubbers, moisture trap). Then it is injected at the bottom of the reactor, either separately or with steam depending on the experimental conditions. A downstream gas pump was operated at a flow range of 0.5–0.6 Nm^3/h to maintain the flow of producer gas through the reactor. A gas meter, placed before the reformer outlet, was used to measure the total amount of gas flowing through the system.

The first stage of this experimental campaign investigates the impact of thermal cracking (TC) on tar removal by feeding the syngas to the tar reformer without a char bed at 750 °C. Once the baseline is determined, any additional tar removal will be attributed to the introduced char and reforming environment. All experiments performed with char bed were at 750 °C and either in the absence (DR: dry reforming) or presence (SR: steam reforming) of two steam levels. Steam is mixed with producer gas by introducing steam at the following flows: 0.02 and 0.18 kg/h, for SR1 and SR2 cases, respectively. Typically, syngas produced from biomass has a steam content in the range of 10–60 vol% [33]. In addition, water is commonly used in the gasification stage to aid in gas conversion and regulate process temperature. However, in the present study, no water was added during the gasification process and the chosen steam levels simulate the upper and lower ranges of typical syngas stream content. A summary of test conditions is shown in Table 1.

Production of gases inside the reactor as a result of reforming reactions also affected the flow through it. Mass balance calculations were solved to obtain the actual flow of producer gas at the inlet of the reactor and the molar flows of single gas species. The residence time was calculated based on the gas hourly space velocity (GHSV) inside the reactor. It varied between 4.2 and 4.7 s for the runs with a char bed. At the end of each run, the flow of producer gas to the reactor was terminated and the electric furnace was turned off. N_2 was continuously flown through the char bed as it was left to cool down. The reactor was then opened, and the char bed was stored for further analysis.

2.4. Gas sampling and analysis

The producer gas was analyzed online using two μGCs (Agilent 490) equipped with two columns: a CP-Molesieve 5 Å and a PoraPLOT-U. The μGCs were pre-calibrated with calibration cylinders (Air Liquide) filled with H_2, CO, CO_2, N_2, and CH_4. Supelclean™ LC-NH2 solid-phase extraction (SPE) tubes weighing 500 mg (3 mL bed volume) were used for tar sampling. Sampling locations are indicated as points A and B in Fig. 1. SPE sampling was made at minute 0, 20, 50, and 110 over the 2 h test. The tube was connected to a 100 mL syringe on one end and a needle (by BRAUN Sterican® 20 G × 2 ¾“) on the other end. The needle was inserted at a sampling port upstream and downstream of the tar reformer to sample the tar in the producer gas. Previous studies showed that drawing 300 mL of producer gas through the adsorbents was sufficient [37], and it was selected for this current study. Before sampling, the tubes were conditioned by passing 5-bed volumes or 1500 μL of dichloromethane through the sorbent material to remove any organic compounds that would bleed into the tar samples [38]. Then it was dried for 5 min at 125 °C [39].

Tar extraction was carried out by passing 1500 μL of dichloromethane through the SPE tube. This was followed by the addition of two internal standards, 100 μL of an aromatic internal standard (*tert*-butylcyclohexane) and 100 μL of a phenolic internal standard (4-ethoxyphenol). The chromatographic detectors were calibrated using benzene, toluene, and naphthalene [38–40]. The three compounds corresponded to the largest peaks on the chromatogram. Moreover, previous work on the open-top gasifier showed that the generated tar was composed mainly of light aromatic compounds, where benzene and toluene accounted for almost 70 % of the total detected tar [41]. Finally, the collected SPE samples were stored in ice before analyzing on the same day. In addition to SPE samples, total tar from the entire run was collected using isopropyl alcohol bubblers (cold trap).

2.5. Gravimetric tar

Gravimetric tars were measured using cold solvent trapping method through CEN/TS 15439: 2006 standard [42]. In brief, a known amount of gas is drawn through six impinger bottles, five of which are filled with isopropanol (IPA) while the last bottle is left empty. Half of the bottles

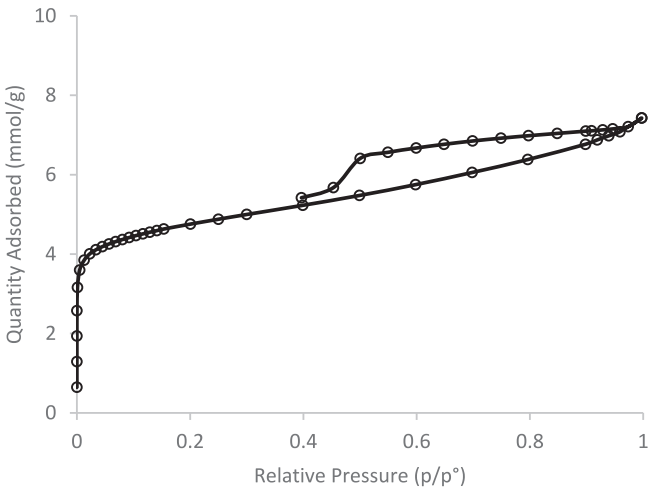

Fig. 2. N_2 adsorption–desorption isotherm of raw char.

Table 2
Overview of raw char XRF results.

P	K	Ca	Mn	Fe	Traces
mg/kg					
732	4880	14,640	2196	732	830

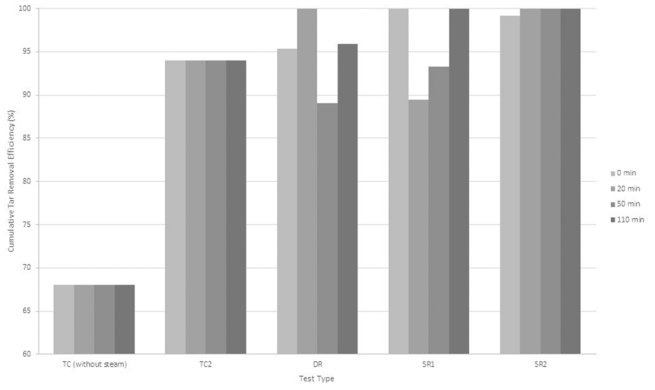

Fig. 3. The combined removal efficiency of selected tar compounds and different time instances.

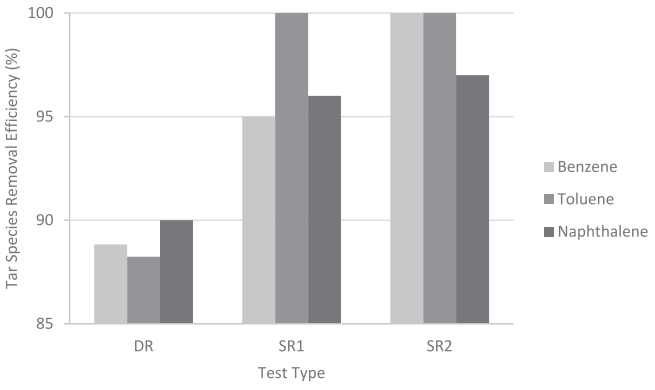

Fig. 4. The removal efficiency of selected tar compounds at different steam volumetric percentages.

are placed in a heated bath and the other half is in an ice bath. Bottle 6 is left empty acting as a droplet collector. When the gas collection is over, all bottles are emptied, while tubing and glass parts are washed with IPA solution. The resulting IPA and tars solution is then placed in a rotavapor to evaporate the IPA solution and the evaporation residue is weighed resulting in the amount of gravimetric tar in mg/Nm^3.

3. Results & discussion

3.1. Char characterization

Before the tar reforming experiment, the open-top resulting char – referred to as "raw char" in the following – was characterized for its moisture, VM, FC, ash, carbon, as well as CHNSO content. The surface properties of the char were also analyzed. The proximate analysis shows that the open-top gasifier produces char with high fixed carbon (93.1 ± 0.5 wt%) and low ash (2.26 ± 0.06 wt%) content. The BET surface area of char, 398 $m^2\ g^{-1}$, is close to the lower end of activated carbon surface area which ranges from 500 to 1500 $m^2\ g^{-1}$ [43]. This is a promising indicator given that the raw char did not go through any type of activation and was not purposely designed for adsorption applications. A closer look at the adsorption isotherms presented in Fig. 2 shows rapid nitrogen adsorption that increases with pressure at the low-pressure region $p/p^\circ \leq 0.1$, indicating the filling of micropores. According to the International Pure and Applied Chemistry (IUPAC) classification, the features of the raw char adsorption–desorption curve show a type H4 hysteresis loop where the adsorption branch resembles a combined type I and II. The increase of adsorbed volume at high relative pressure suggests the presence of macropores that are not completely filled with pore condensate [44].

The mesopore volume (0.110 $cm^3\ g^{-1}$) and micropore volume (0.164 $cm^3\ g^{-1}$) obtained through BJH, and HK analysis, respectively, show a large percentage (60 %) of micropores. In comparison, 40 % of mesopores were present. Unlike micropores, mesopores do not contribute very much to initial tar conversion. However, they are more resilient and could decrease the char deactivation rate [45]. Surface functional groups such as carboxylic acid or carbonylic groups are known to have an impact on the char catalytic properties [46]. Nevertheless, the high temperature experienced at the open-top gasifier reaching almost 1100 °C reduces the oxygen content in the char severely. Thus, the influence of oxygen functional groups, if present, is not significant. Table 2 shows the most abundant inorganic elements in the raw char. The char is rich in Ca, K, and Mn with lower quantities of P, Fe as well as other trace elements. Alkali and alkaline-earth metals (AAEM, mainly Na, Mg, K, and Ca) act as active sites for the conversion of adsorbed tar compounds into lighter components [47].

3.2. Effect of reforming on tar and gaseous species concentrations

Tar reforming experiments were conducted at 750 °C which should be sufficient to reach tar conversion rates above 90 % in the presence of a gasifying agent (i.e., H_2O) [48]. The producer gas used in this experiment has a relatively low tar content due to the different cleaning stages at the open-top gasifier before feeding into the tar reformer. The expected tars are light aromatics and polyaromatics of class III and IV, respectively, according to ECN tar classes [49]. At the reformer inlet, the benzene, toluene, and naphthalene concentration measured using SPE were 1634 ± 42 mg/Nm^3, 614 ± 32 mg/Nm^3, and 157 ± 5 mg/Nm^3, respectively. Moreover, the inlet gas temperature was around 30 °C. In the case of TC (without steam), the total tar removal efficiency was the lowest at 68 %, without showing significative variations with time due to a steady-state effect of thermal cracking alone. When thermal cracking was performed at the highest steam level (TC2), the cumulative tar removal efficiency was 94 %. As shown in Fig. 3, introducing the char bed without steam (DR) results in an initial total removal efficiency of 95 %, which reaches a maximum of 100 % after 20 min. Then, the

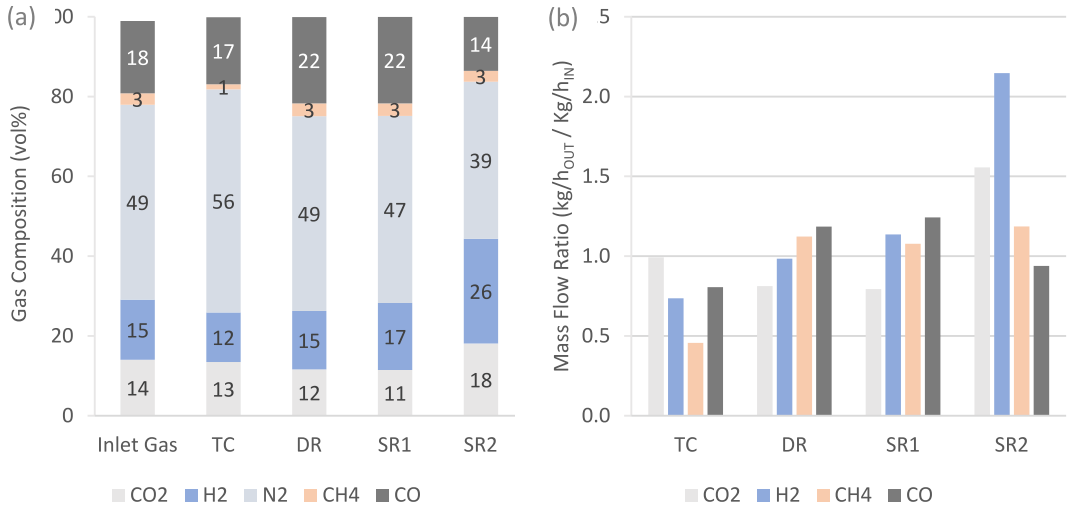

Fig. 5. A) Gas composition at the reformer inlet and outlet, and b) mass flow ratio of gaseous species. (colored).

Table 3
Proximate and ultimate analysis of raw and spent chars.

	VM	FC	Ash	C	H	N	O*
	wt_{dry}%						
Raw Char	4.9 ± 1.4	93.1 ± 0.5	2.0 ± 1.9	94.85 ± 0.34	0.72 ± 0.04	0.50 ± 0.01	1.49
DR	3.2 ± 0.3	94.3 ± 0.3	2.5 ± 0.1	94.73 ± 1.57	0.61 ± 0.01	0.54 ± 0.01	1.82
SR1	4.4 ± 0.1	92.6 ± 0.5	3.0 ± 0.4	94.84 ± 0.49	0.56 ± 0.01	0.61 ± 0.03	1.51
SR2	3.3 ± 0.4	94.3 ± 0.4	2.3 ± 0.1	94.63 ± 0.51	0.63 ± 0.02	0.45 ± 0.04	1.80

*By difference.
The sulfur amount is less than 0.2 % for all samples.

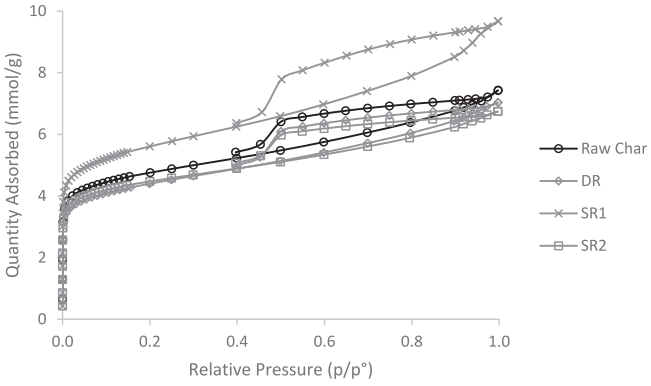

Fig. 6. N_2 adsorption isotherms comparing raw and spent chars.

Table 4
Raw and spent chars' surface properties obtained with N_2 adsorption at 77 K.

	BET Surface Area	Total Pore Volume	Mesopore Volume		Micropore Volume	
			Barrett-Joyner-Halenda (BJH)		Horvath–Kawazoe (HK)	
	$m^2\ g^{-1}$	$cm^3\ g^{-1}$	$cm^3\ g^{-1}$	%	$cm^3\ g^{-1}$	%
Raw Char	398	0.274	0.110	40	0.164	60
DR	366	0.270	0.118	44	0.152	56
SR1	465	0.361	0.168	47	0.193	53
SR2	376	0.238	0.084	35	0.154	65

Table 5
Mass loss of the char bed at the end of the 2 h reforming tests.

	Initial bed weight (g)	Final bed weight (g)	Mass loss (%)
	g	g	%
DR	600	578.5	3.6
SR1	600	575.1	4.2
SR2	600	537.2	10.5

removal efficiency decreases at 50 min followed by an increase at the end of the test (96 % at 110 min). A similar cyclic effect it observed at the first steam level (SR1) with a major difference: at min 0, the total removal efficiency was already 100 %, then it decreases to 89 % followed by an upward trend. Although only attributed to the presence of steam and the related opening up of the pores, cyclic behavior was observed in the DR case suggesting a higher inherent moisture content in the producer gas. At SR2, tar removal efficiency is instead almost constant and the cyclic effect is no longer observed. The lowest removal efficiency experienced at the start of the SR2 case corresponds to a tar concentration of 20 mg/Nm^3. The higher steam percentage is responsible for char regeneration and this allows for maintaining its catalytic activity throughout the test [50]. It also results in a larger fraction of steam reforming as shown in Fig. 3. The impact of the char bed on tar reforming is clear when comparing the TC (without steam) to DR cases. Moreover, TC2 (0.18 kg/h steam) showed a comparable performance to the case of DR (without steam) and SR1 (0.02 kg/h steam). From this we can conclude that using char, either without steam or with very low steam concentration, can reduce the energy demand for steam generation while achieving the same tar removal efficiency.

Between the three studied compounds, catalytic cracking of toluene at 750 °C seemed unaffected by steam level as shown in Fig. 4. Other studied tar compounds showed an improved removal efficiency with increasing steam level. In addition to the tar reforming effect, introducing the char bed at the second steam level, resulted in an increase of H_2 production from 15 vol% to 26 vol% as shown in Fig. 5. This is an indicator of an increased steam reforming of tars (reaction (1) as well as

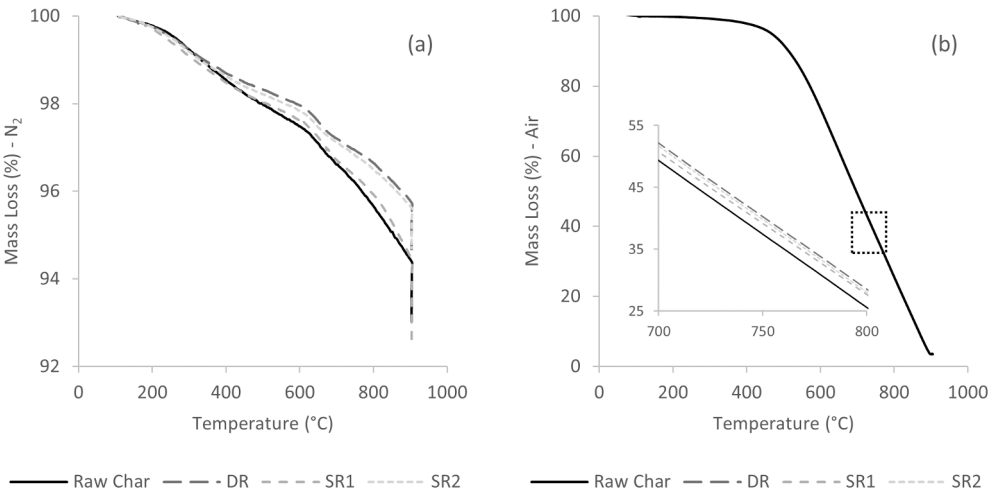

Fig. 7. Mass loss curves of raw and spent chars in (a) N_2 and (b) synthetic air environments.

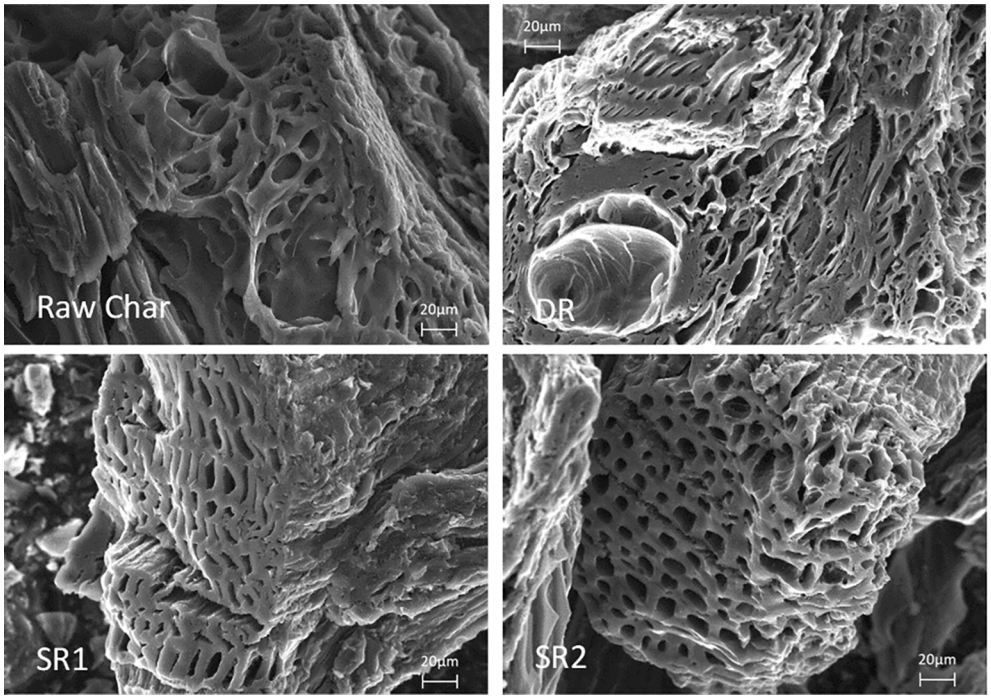

Fig. 8. SEM images showing the microstructure of the raw char and spent chars (DR, SR1, and SR2).

water–gas shift reaction (reaction (5). The mass flow ratio of gaseous species at the reformer was also calculated from the ratio of inlet and outlet mass flows (kg/h) of H_2, CO, CO_2, and CH_4. The impact of steam is noticeably higher for H_2 at SR2 which indicates an increased rate of char gasification (reaction (6) correlated with the higher char bed mass loss (10.5 %).

$$CO + H_2O \leftrightarrow CO_2 + H_2 \quad (5)$$

$$C\ (char) + H_2O \rightarrow H_2 + CO \quad (6)$$

The measured gravimetric tar before the reformer was 2407 mg/Nm^3. This value falls within the expected tar range of downdraft gasifier which spans from 0.01 to 6 g/Nm^3 [22]. Downdraft gasifiers are marked by their low tar concentration as the producer gas passes through the highest temperature zone before exiting the gasifier. As a result, only lighter tar compounds (ECN class II-IV) are expected. A more detailed gravimetric tar analysis of the open-top gasifier conducted previously showed that benzene and toluene constituted 70 % of the quantified tars, followed by styrene, phenol, and naphthalene [41]. The gravimetric analysis makes it possible to capture all tar components except the very volatile ones. A detailed comparison of the SPE and gravimetric tar methods for a fluidized bed gasifier showed a big discrepancy between the sum of GC-detectable tars measured with SPE and gravimagnetic tars [51]. Nevertheless, the specific tar distribution strongly depends on the type of gasifier. In the present study, due to the absence of heavy tars, SPE and gravimetric tar values were in agreement. It was also shown in previous work that SPE and gravimetric tars are in agreement when considering benzene, toluene, and m/p-xylene regardless of the gasifier type [51].

3.3. *Effect of tar reforming on char properties*

The comparison of raw and spent char in terms of VM, FC, and ash content as well as the elemental analysis reveals no significant

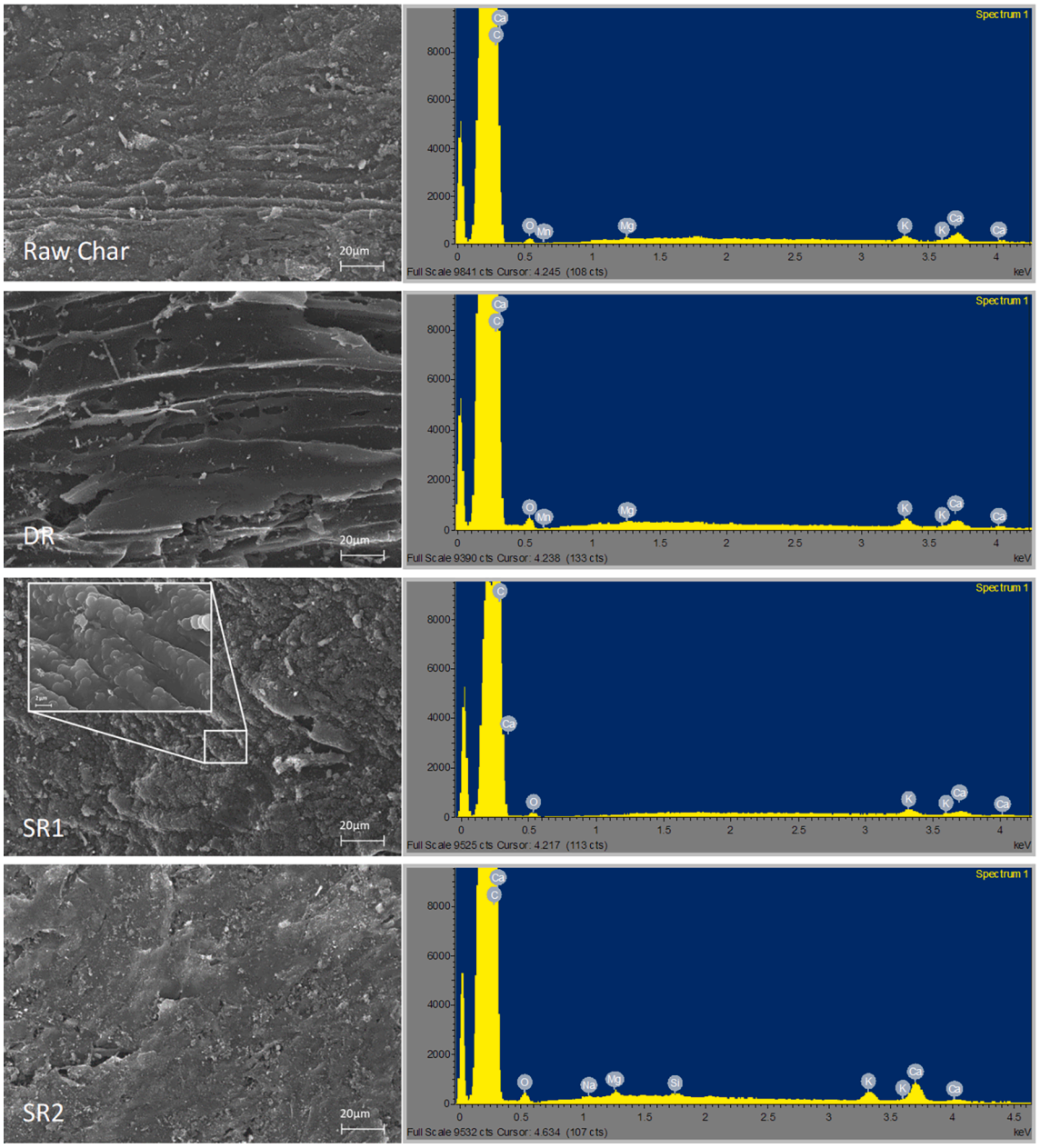

Fig. 9. SEM images with EDX spectra of the raw char and spent chars (DR, SR1, and SR2).

differences between the char properties before and after the reforming experiments as shown in Table 3. Physical and thermal analysis is therefore recommended.

In terms of surface properties, shown in Table 4, the surface area of char has decreased as a result of the tar reforming process for the cases DR and SR2. It is expected to observe such a trend due to pore clogging with coke during the reforming process [52,53]. However, at the lower steam level (SR1) an increase in surface area was observed. This is likely due to the presence of appropriate steam concentration for char activation in combination with the large bed size, short test duration, and low initial tar concentration. The observed phenomena are related to the physical activation of carbonaceous materials with steam. To achieve good pore development, steam should react inside the pores at an appropriate rate relative to the release of reaction products [54]. In other words, the increased production of CO_2 and H_2 due to char gasification reactions at the interior of the char particles will inhibit further pore development, and favor the reaction of steam at the char surface [55]. This was evident in the increased mass loss, 10.5 % compared to 4.2 %, for SR1 and SR2 cases, respectively (Table 5), as well as the increased H_2 production (Fig. 5). The isotherms in Fig. 6 show a larger hysteresis loop and steeper adsorption curve for SR1 spent char, indicating a larger percentage of mesopores compared to raw char, DR and SR2 spent chars.

Thermal degradation of raw and spent char samples in N_2 and synthetic air atmospheres is shown in Fig. 7. In N_2, the thermal degradation of raw char was the fastest followed by SR1 and SR2 spent chars. The slowest degradation was observed in DR spent char. In air, a similar trend was observed where spent char had a slower degradation compared to raw char. A slower thermal degradation is typically correlated with a higher degree of deactivation [36]. Unlike raw char, spent char possibly has more condensed tar compounds on its surface that accumulate during the reforming process.

The rsults of the SEM-EDX analysis are given in Fig. 8 and Fig. 9. It can be seen that both raw and spent chars had well developed porosity with no severe clogging of the pores. This was likely possible due to the large bed size and short reforming test. The EDX spectra in Fig. 9 show a

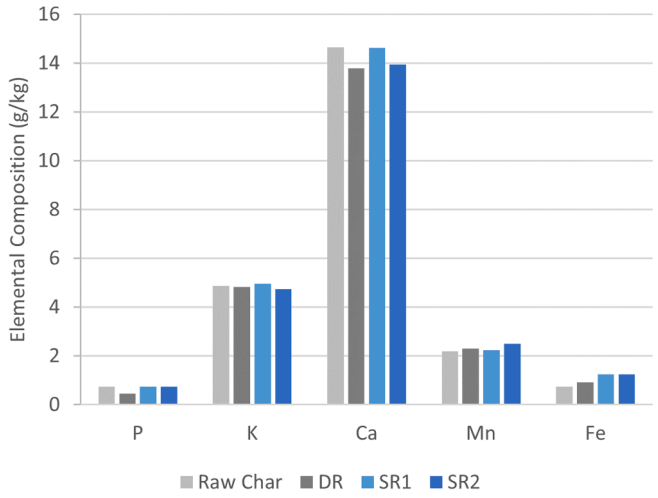

Fig. 10. Summary of the main inorganic elements in raw and spent chars samples. (colored).

Table 6
Summary of PAH analysis results.

	Raw Char	DR	SR1	SR2
	mg/kg			
Fluoranthene	< 0.1	< 0.1	< 0.1	< 0.1
Benzo(*b*)fluoranthene	< 0.1	< 0.1	< 0.1	< 0.1
Benzo(*k*)fluoranthene	< 0.1	< 0.1	< 0.1	< 0.1
Benzo(*a*)pyrene	< 0.1	< 0.1	< 0.1	< 0.1
Benzo(*g,h,i*)perylene	< 0.1	< 0.1	< 0.1	< 0.1
Indeno(*1,2,3cd*)pyrene	< 0.1	< 0.1	< 0.1	< 0.1
Anthracene	< 0.1	< 0.1	< 0.1	< 0.1
Acenaphthene	< 0.1	< 0.1	< 0.1	< 0.1
Chrysene	< 0.1	< 0.1	< 0.1	< 0.1
Dibenzo(*a,h*)anthracene	< 0.1	< 0.1	< 0.1	< 0.1
Fluorene	< 0.1	< 0.1	< 0.1	< 0.1
Naphthalene	1.05	< 0.1	0.11	0.15
Pyrene	< 0.1	< 0.1	< 0.1	< 0.1
Phenanthrene	< 0.1	< 0.1	< 0.1	< 0.1
Acenaphthylene	< 0.1	< 0.1	< 0.1	< 0.1
Benzo(*a*)anthracene	< 0.1	< 0.1	< 0.1	< 0.1
Sum of 16 EPA PAH	< 2.550	< 1.600	< 1.610	< 1.615
Detection limit = 0.1 mg/kg				

good mineral dispersion with homogeneous particle sizes. The most abundant minrals on the char surface were Mg, K, and Ca. Fig. 9 also shows nicely the soot on the spent char SR1 as well as the increased O and Ca counts on spent char SR2 surface which is probably due to the higher steam concentration.

Fig. 10 presents the results of XRF analysis for raw and spent char samples. An observed increase in the concentration of certain elements such as Fe can be a result of a faster char gasification rate in comparison to the loss of inorganic elements. A decrease in some AAEM (mainly K and Ca) elements concentration is expected although not observed in XRF analysis results due to its semiquantitative nature. The AAEMs in gasification char are typically in the form of inorganic salts, and they may be decomposed to a gaseous phase at high temperatures [56,57]. Also at elevated temperatures, the silicon existing in the char could form alkali silicates which inhibit the catalytic effect of AAEM species in tar reforming reactions [58,59]. Silicon content is typically low in woody biomass [47]. As a result, its inhibitory effect can be neglected in this study. It is also possible that the mineral content increase after the reforming tests due to the gasification of char and the consequent concentration effect. This could impact the future use of char in certain applications (e.g., water treatment) were a limit on the mineral content exists. However, in this study no change in mineral content was observe.

Concerning PAH contamination, Table 6 summarizes the 16 EPA PAH content in raw and spent chars. Those PAH are regulated for soil application. All chars had relatively low PAH content that is below the lower limit indicated by the European Biochar Certificate for soil application (6 mg/kg) [60]. Compared to raw char, spent chars had lower PAH content, which is consistent with previous work [36].

4. Conclusions

Tar reforming at a pilot scale was conducted using a char bed and steam generator for the purpose of cleaning the producer gas as well as upgrading it. An open-top downdraft gasifier operated with wood pellets as feedstock supplied both producer gas as well as raw char. Tar quantification through gravimetric analysis and SPE at the open-top gasifier outlet (reformer inlet) showed that tar concentration falls within the expected range for downdraft gasifier, 0.01–6 g/Nm^3 [22]. However, further cleaning is needed for syngas production [61]. The impact of the char bed was studied in relation to the thermal cracking case. In addition to dry reforming, steam reforming was performed at 0.02 and 0.18 kg/h steam. Raw and spent char properties were finally compared to evaluate possible post-reforming utilization routes.

The results showed a significant reduction in tar concentration for all reforming cases in comparison to the thermal cracking condition. Tar removal efficiency increased from 68 % to nearly 100 % for the TC, and SR2 cases, respectively. The cyclic behavior of char activation and deactivation was observed in both DR and SR1 cases. At the different sampling intervals and when a char bed was used, tar concentration was around or above 90 %. Physical and chemical characterization of raw and spent char showed no significant impact of the reforming tests on char qualities and the bed can be still used for extended periods before replacement. The only difference observed was the improved surface properties of SR1 spent char which showed an increase in both surface area and pore volume. The lower PAH content in spent char in comparison to the raw char makes it a promising material for urban (carbon storage) and agricultural applications. From a wider perspective, gasification char utilization in tar reforming creates value from waste and achieves circularity. It also upgrades the producer gas using a catalyst readily available. It is worth noting that char was used as-received without modification. Nevertheless, it showed an excellent tar reforming performance.

Future work should focus on the implementation of gasification char generated at a commercial scale which is often in powder form due to the higher conversion rates. Powders impose a challenge when used in fixed bed due to the significant pressure drop created. Efforts should be made to put this char in a suitable form for tar reforming. Finally, gasification char was found in many other applications, notably, wastewater treatment which could also benefit from a pelletized char.

CRediT authorship contribution statement

Ali Abdelaal: Conceptualization, Data curation, Formal analysis, Investigation, Methodology, Visualization, Writing – original draft, Writing – review & editing. **Daniele Antolini:** Data curation, Investigation, Methodology. **Stefano Piazzi:** Data curation, Investigation, Methodology, Writing – review & editing. **Francesco Patuzzi:** Conceptualization, Funding acquisition, Methodology, Resources, Supervision, Writing – review & editing. **Audrey Villot:** Conceptualization, Methodology, Resources, Supervision, Writing – review & editing, Funding acquisition. **Claire Gerente:** Conceptualization, Resources, Supervision, Writing – review & editing, Funding acquisition. **Marco Baratieri:** Conceptualization, Funding acquisition, Methodology, Resources, Supervision, Writing – review & editing.

Declaration of Competing Interest

The authors declare that they have no known competing financial

interests or personal relationships that could have appeared to influence the work reported in this paper.

Data availability

Data will be made available on request.

Acknowledgment

The authors would like to thank Dr. Benedetti Vittoria and Dr. Eleonora Cordioli from the Free University of Bozen-Bolzano, and Mr. Valentin Damour from Institut des Matériaux de Nantes for their support with material characterization and tar analysis.

References

[1] Cazzaniga NE, Jasinevičius G, Mubareka S. Sankey diagrams of woody biomass flows in the European Union - 2021 release. 2022.
[2] Molino A, Chianese S, Musmarra D. Biomass gasification technology: the state of the art overview. J Energy Chem 2016;25:10–25. https://doi.org/10.1016/J.JECHEM.2015.11.005.
[3] Piazzi S, Patuzzi F, Baratieri M. Energy and exergy analysis of different biomass gasification coupled to Fischer-Tropsch synthesis configurations. Energy 2022;249:123642. https://doi.org/10.1016/J.ENERGY.2022.123642.
[4] Benedetti V, Ail SS, Patuzzi F, Cristofori D, Rauch R, Baratieri M. Investigating the feasibility of valorizing residual char from biomass gasification as catalyst support in Fischer-Tropsch synthesis. Renew Energy 2020;147:884–94. https://doi.org/10.1016/j.renene.2019.09.050.
[5] Ren J, Liu YL, Zhao XY, Cao JP. Methanation of syngas from biomass gasification: an overview. Int J Hydrogen Energy 2020;45:4223–43. https://doi.org/10.1016/J.IJHYDENE.2019.12.023.
[6] Piazzi S, Menin L, Antolini D, Patuzzi F, Baratieri M. Potential to retrofit existing small-scale gasifiers through steam gasification of biomass residues for hydrogen and biofuels production. Int J Hydrogen Energy 2021;46:8972–85. https://doi.org/10.1016/j.ijhydene.2021.01.004.
[7] Hrbek J. Status report on thermal gasification of biomass and waste. 2019. https://doi.org/978-1-910154-65-6.
[8] Patuzzi F, Basso D, Vakalis S, Antolini D, Piazzi S, Benedetti V, et al. State-of-the-art of small-scale biomass gasification systems: an extensive and unique monitoring review. Energy 2021;223:120039. https://doi.org/10.1016/j.energy.2021.120039.
[9] Bain RL, Broer K. Chapter 3: Gasification. In: Brown RC, editor. Thermochem. Process. Biomass Convers. into Fuels, Chem. Power, John Wiley & Sons, Ltd; 2011, p. 47–77. https://doi.org/https://doi.org/10.1002/9781119990840.ch3.
[10] Hansen V, Müller-Stöver D, Ahrenfeldt J, Holm JK, Henriksen UB, Hauggaard-Nielsen H. Gasification biochar as a valuable by-product for carbon sequestration and soil amendment. Biomass Bioenergy 2015;72:300–8. https://doi.org/10.1016/j.biombioe.2014.10.013.
[11] Shackley S, Carter S, Knowles T, Middelink E, Haefele S, Sohi S, et al. Sustainable gasification–biochar systems? A case-study of rice-husk gasification in Cambodia, Part I: context, chemical properties, environmental and health and safety issues. Energy Policy 2012;42:49–58. https://doi.org/10.1016/J.ENPOL.2011.11.026.
[12] Brewer CE, Unger R, Schmidt-Rohr K, Brown RC. Criteria to select biochars for field studies based on biochar chemical properties. BioEnergy Res 2011;4:312–23. https://doi.org/10.1007/s12155-011-9133-7.
[13] Wiedner K, Rumpel C, Steiner C, Pozzi A, Maas R, Glaser B. Chemical evaluation of chars produced by thermochemical conversion (gasification, pyrolysis and hydrothermal carbonization) of agro-industrial biomass on a commercial scale. Biomass Bioenergy 2013;59:264–78. https://doi.org/10.1016/j.biombioe.2013.08.026.
[14] Buentello-Montoya DA, Zhang X, Li J. The use of gasification solid products as catalysts for tar reforming. Renew Sustain Energy Rev 2019;107:399–412. https://doi.org/10.1016/j.rser.2019.03.021.
[15] Antolini D, Piazzi S, Menin L, Baratieri M, Patuzzi F. High hydrogen content syngas for biofuels production from biomass air gasification: experimental evaluation of a char-catalyzed steam reforming unit. Int J Hydrogen Energy 2022;47:27421–36. https://doi.org/10.1016/J.IJHYDENE.2022.06.075.
[16] Ren J, Cao JP, Zhao XY, Liu YL. Fundamentals and applications of char in biomass tar reforming. Fuel Process Technol 2021;216:106782. https://doi.org/10.1016/j.fuproc.2021.106782.
[17] Cha JS, Park SH, Jung S-C, Ryu C, Jeon J-K, Shin M-C, et al. Production and utilization of biochar: a review. J Ind Eng Chem 2016;40:1–15. https://doi.org/10.1016/j.jiec.2016.06.002.
[18] Lee J, Kim KH, Kwon EE. Biochar as a catalyst. Renew Sustain Energy Rev 2017;77:70–9.
[19] Cordioli E, Patuzzi F, Baratieri M. Thermal and catalytic cracking of toluene using char from commercial gasification systems. Energies 2019;12. https://doi.org/10.3390/en12193764.
[20] Abdelaal A, Benedetti V, Villot A, Patuzzi F, Gerente C, Baratieri M. Innovative pathways for the valorization of biomass gasification char: a systematic review. Energies 2023;16:4175. https://doi.org/10.3390/en16104175.
[21] Speight JG. Handbook of gasification technology: science, technology, and processes. Wiley-Scrivener; 2020.
[22] Basu P. Chapter 6: Tar Production and Destruction. Biomass Gasification, Pyrolysis and Torrefaction, Elsevier; 2013, p. 177–98. https://doi.org/10.1016/b978-0-12-396488-5.00006-x.
[23] Shen Y. Chars as carbonaceous adsorbents/catalysts for tar elimination during biomass pyrolysis or gasification. Renew Sustain Energy Rev 2015;43:281–95. https://doi.org/10.1016/j.rser.2014.11.061.
[24] Dufour A. Molecular Scale. Thermochem. Convers. Biomass Energy Chem. Prod., Hoboken, USA: John Wiley & Sons, Inc.; 2016, p. 93–134. https://doi.org/10.1002/9781119137696.
[25] Kirchherr J, Reike D, Hekkert M. Conceptualizing the circular economy: an analysis of 114 definitions. Resour Conserv Recycl 2017;127:221–32. https://doi.org/10.1016/J.RESCONREC.2017.09.005.
[26] Pio DT, Tarelho LAC. Industrial gasification systems (>3 MWth) for bioenergy in Europe: current status and future perspectives. Renew Sustain Energy Rev 2021;145:111108. https://doi.org/10.1016/j.rser.2021.111108.
[27] European Biogas Association. Gasification – A Sustainable Technology for Circular Economies. Brussels: 2021.
[28] Arora S, Jung J, Liu M, Li X, Goel A, Chen J, et al. Gasification biochar from horticultural waste: an exemplar of the circular economy in Singapore. Sci Total Environ 2021;781:146573. https://doi.org/10.1016/j.scitotenv.2021.146573.
[29] Assima GP, Marie-Rose S, Lavoie JM. Role of fixed carbon and metal oxides in char during the catalytic conversion of tar from RDF gasification. Fuel 2018;218:406–16. https://doi.org/10.1016/j.fuel.2017.12.039.
[30] Assima GP, Paquet A, Lavoie J. Utilization of MSW-derived char for catalytic reforming of Tars and light hydrocarbons in the primary syngas produced during wood chips and MSW-RDF air gasification. Waste Biomass Valoriz 2019;10:1203–22. https://doi.org/10.1007/s12649-017-0138-0.
[31] Singh S, Kumar Bhaumik S, Dong L, Li CZ, Vuthaluru H. An integrated two-step process of reforming and adsorption using biochar for enhanced tar removal in syngas cleaning. Fuel 2022;307:121935. https://doi.org/10.1016/J.FUEL.2021.121935.
[32] Korus A, Ravenni G, Loska K, Korus I, Samson A, Szlęk A. The importance of inherent inorganics and the surface area of wood char for its gasification reactivity and catalytic activity towards toluene conversion. Renew Energy 2021;173:479–97. https://doi.org/10.1016/j.renene.2021.03.130.
[33] Cheng L, Wu Z, Zhang Z, Guo C, Ellis N, Bi X, et al. Tar elimination from biomass gasification syngas with bauxite residue derived catalysts and gasification char. Appl Energy 2020;258:114088. https://doi.org/10.1016/j.apenergy.2019.114088.
[34] Parrillo F, Ruoppolo G, Arena U. The role of activated carbon size in the catalytic cracking of naphthalene. Energy 2020;190:116385. https://doi.org/10.1016/j.energy.2019.116385.
[35] Frainetti AJ, Klinghoffer NB. Recent experimental advances on the utilization of biochar as a tar reforming catalyst: a review. Int J Hydrogen Energy 2023;48(22):8022–44. https://doi.org/10.1016/J.IJHYDENE.2022.11.127.
[36] Ravenni G, Sárossy Z, Sanna S, Ahrenfeldt J, Henriksen UB. Residual gasification char applied to tar reforming in a pilot-scale gasifier: performance and evolution of char properties for perspective cascade uses. Fuel Process Technol 2020;210:106546. https://doi.org/10.1016/j.fuproc.2020.106546.
[37] Osipovs S. Use of two different adsorbents for sampling tar in gas obtained from peat gasification. Int J Environ Anal Chem 2009;89:871–80. https://doi.org/10.1080/03067310802592755.
[38] Horvat A, Kwapinska M, Abdel Karim Aramouni N, Leahy JJ. Solid phase adsorption method for tar sampling – How post sampling treatment affects tar yields and volatile tar compounds? Fuel 2021;291:120059. https://doi.org/10.1016/j.fuel.2020.120059.
[39] Brage C, Yu Q, Chen G, Sjöström K. Use of amino phase adsorbent for biomass tar sampling and separation. Fuel 1997;76:137–42. https://doi.org/10.1016/S0016-2361(96)00199-8.
[40] Israelsson M, Seemann M, Thunman H. Assessment of the solid-phase adsorption method for sampling biomass-derived tar in industrial environments. Energy Fuel 2013;27:7569–78. https://doi.org/10.1021/ef401893j.
[41] Prando D, Shivananda Ail S, Chiaramonti D, Baratieri M, Dasappa S. Characterisation of the producer gas from an open top gasifier: assessment of different tar analysis approaches. Fuel 2016;181:566–72. https://doi.org/10.1016/J.FUEL.2016.04.104.
[42] CEN/TS 15439:2006. Biomass gasification – tar and particles in product gases – sampling and analysis. Eur Comm Stand 2006.
[43] Ferhan C, Ozgur A. Activated carbon for water and wastewater treatment: integration of adsorption and biological treatment. Weinheim: Wiley-VCH; 2011.
[44] Thommes M, Kaneko K, Neimark AV, Olivier JP, Rodriguez-Reinoso F, Rouquerol J, et al. Physisorption of gases, with special reference to the evaluation of surface area and pore size distribution (IUPAC Technical Report). Pure Appl Chem 2015;87:1051–69. https://doi.org/10.1515/pac-2014-1117.
[45] Hervy M, Weiss-Hortala E, Pham Minh D, Dib H, Villot A, Gérente C, et al. Reactivity and deactivation mechanisms of pyrolysis chars from bio-waste during catalytic cracking of tar. Appl Energy 2019;237:487–99. https://doi.org/10.1016/j.apenergy.2019.01.021.
[46] Rodríguez-Reinoso F. The role of carbon materials in heterogeneous catalysis. Carbon N Y 1998;36:159–75. https://doi.org/10.1016/S0008-6223(97)00173-5.
[47] Shrestha P, Chun DD, Kang K, Simson AE, Klinghoffer NB. Role of metals in biochar production and utilization in catalytic applications: a review. Waste Biomass Valoriz 2022;13(2):797–822. https://doi.org/10.1007/s12649-021-01519-6.
[48] Ravenni G, Sárossy Z, Ahrenfeldt J, Henriksen UB. Activity of chars and activated carbons for removal and decomposition of tar model compounds – A review.

Renew Sustain Energy Rev 2018;94:1044–56. https://doi.org/10.1016/j.rser.2018.07.001.
[49] Rabou LPLM, Zwart RWR, Vreugdenhil BJ, Bos L. Tar in biomass producer gas, the energy research centre of The Netherlands (ECN) experience: an enduring challenge. Energy Fuel 2009;23:6189–98. https://doi.org/10.1021/ef9007032.
[50] Morin M, Nitsch X, Hémati M. Interactions between char and tar during the steam gasification in a fluidized bed reactor. Fuel 2018;224:600–9. https://doi.org/10.1016/j.fuel.2018.03.050.
[51] Neubert M, Reil S, Wolff M, Pöcher D, Stork H, Ultsch C, et al. Experimental comparison of solid phase adsorption (SPA), activated carbon test tubes and tar protocol (DIN CEN/TS 15439) for tar analysis of biomass derived syngas. Biomass Bioenergy 2017;105:443–52. https://doi.org/10.1016/j.biombioe.2017.08.006.
[52] Buentello-Montoya D, Zhang X, Li J, Ranade V, Marques S, Geron M. Performance of biochar as a catalyst for tar steam reforming: Effect of the porous structure. Appl Energy 2020;259:114176. https://doi.org/10.1016/J.APENERGY.2019.114176.
[53] Abdoulmoumine N, Adhikari S, Kulkarni A, Chattanathan S. A review on biomass gasification syngas cleanup. Appl Energy 2015;155:294–307. https://doi.org/10.1016/J.APENERGY.2015.05.095.
[54] Manocha SM, Patel H, Manocha LM. Effect of steam activation parameters on characteristics of pine based activated carbon. Carbon Lett 2010;11:201–5. https://doi.org/10.5714/CL.2010.11.3.201.
[55] Rodríguez-Reinoso F, Molina-Sabio M, González MT. The use of steam and CO_2 as activating agents in the preparation of activated carbons. Carbon N Y 1995;33:15–23. https://doi.org/10.1016/0008-6223(94)00100-E.
[56] Feng D, Zhang Y, Zhao Y, Sun S, Wu J, Tan H. Mechanism of in-situ dynamic catalysis and selective deactivation of H_2O-activated biochar for biomass tar reforming. Fuel 2020;279:118450. https://doi.org/10.1016/J.FUEL.2020.118450.
[57] Long J, Song H, Jun X, Sheng S, Lun-shi S, Kai X, et al. Release characteristics of alkali and alkaline earth metallic species during biomass pyrolysis and steam gasification process. Bioresour Technol 2012;116:278–84. https://doi.org/10.1016/J.BIORTECH.2012.03.051.
[58] Nzihou A, Stanmore B, Sharrock P. A review of catalysts for the gasification of biomass char, with some reference to coal. Energy 2013;58:305–17. https://doi.org/10.1016/J.ENERGY.2013.05.057.
[59] Dupont C, Nocquet T, Da Costa JA, Verne-Tournon C. Kinetic modelling of steam gasification of various woody biomass chars: influence of inorganic elements. Bioresour Technol 2011;102(20):9743–8. https://doi.org/10.1016/J.BIORTECH.2011.07.016.
[60] Schmidt HP, Bucheli T, Kammann C, Glaser B, Abiven S, Leifeld J, et al. Guidelines European Biochar Certificate. vol. 10.1. 2022.
[61] Pena J, Villot A, Gerente C. Pyrolysis chars and physically activated carbons prepared from buckwheat husks for catalytic purification of syngas. Biomass Bioenergy 2020;132:105435. https://doi.org/10.1016/j.biombioe.2019.105435.